EGU General Assembly 2025

EGU25-124

Solar Wind-Mercury's Magnetosphere Interaction by Data Exploration and MHD Simulations

27th April – 2nd May, 2025 Vienna, Austria

Shu-Hua Lai[1], **Yung-Ching Wang**[2], **Ya-Hui Yang**[1,3], and **Wing-Huen Ip**[2,3]

lucky@g.ncu.edu.tw

[1] Center for Astronautical Physics and Engineering, National Central University, Taiwan
[2] Graduate Institute of Astronomy, National Central University, Taiwan
[3] Department of Space Science and Engineering, National Central University, Taiwan

Mercury's magnetosphere is more dynamic than Earth's due to its proximity to the Sun, and it is subject to a lower Mach number solar wind. Regarding the solar wind interaction with Mercury, we are interested in the configurations of Mercury's magnetosphere and the energy transport under various solar wind conditions. First, this study examines the potential impact of low Mach number solar wind on Mercury's bow shock and the resulting effects on the magnetosphere. To analyze the variability of Mercury's bow shock in response to solar wind properties, this study combines observations by the Helios data with theoretical solutions and MHD simulations. The results show that when Mercury encounters solar wind with an extremely low Mach number, its bow shock is expected to become more flattened, further from the planet, and may even disappear, which means the interactions between the solar wind and Mercury's magnetosphere would be anomalies. We also found that Mercury's bow shock would become a concave-upward slow-mode shock. Our other focus is on the Kelvin-Helmholtz instability (KHI) at Mercury's magnetopause, which is crucial in the energy and momentum coupling process between the solar wind and planetary magnetospheres. To investigate this phenomenon, we have conducted MHD simulations using a specific set of boundary conditions and plasma parameters derived from hybrid simulations of the first encounter of the MESSENGER spacecraft with Mercury in 2008. We discovered that a heavily mass-loaded Mercury's magnetosphere allows KHI waves to extract energy and momentum more effectively from the solar wind and transport them into the inner Mercury's magnetosphere when the nonlinear fast-mode plane waves are generated by the fast-mode waves emitted from the KHI surface waves.

Disappearance of Mercury's Bow Shock

Data Exploration: Helios Mission

(Source of this figure is http://solarsystem.nasa.gov/multimedia/display.cfm?IM_ID=10623)

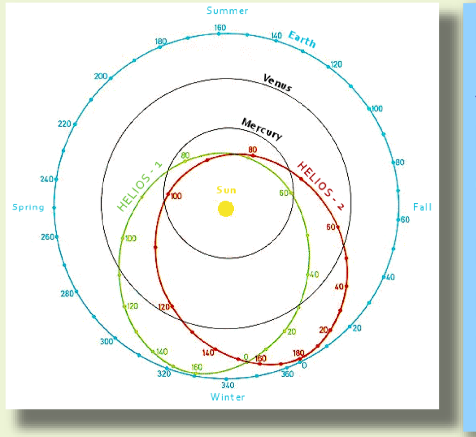

Helios 1/2 orbits:
Aphelion: 0.29AU
Perihelion: 1.0AU
(cover Mercury's orbit)

Mission durations:
Helios 1: 1975/01~1985/02
Helios 2: 1976/07~1979/12
(cover 2/3 solar cycle 21)

Fast-mode Mach number

$$\mathbf{M_F} = \frac{\mathbf{V_{SW}}}{\mathbf{C_F}}$$ (V_{SW}:solar wind speed)

Sound Speed (km/s)

$$\mathbf{C_S} = \sqrt{\frac{\left(\frac{5}{3}\right)\mathbf{P}}{\mathbf{n_p} \times 1.6726}} \times 10^3$$

Alfvén speed (km/s)

$$\mathbf{C_A} = \frac{\mathbf{B} \times 21.8}{\sqrt{\mathbf{n_p}}}$$

Fast-Mode Speed

$$\mathbf{C_F} \approx \sqrt{\mathbf{C_S^2} + \mathbf{C_A^2}}$$

yearly distribution of solar wind properties (PDF plots)

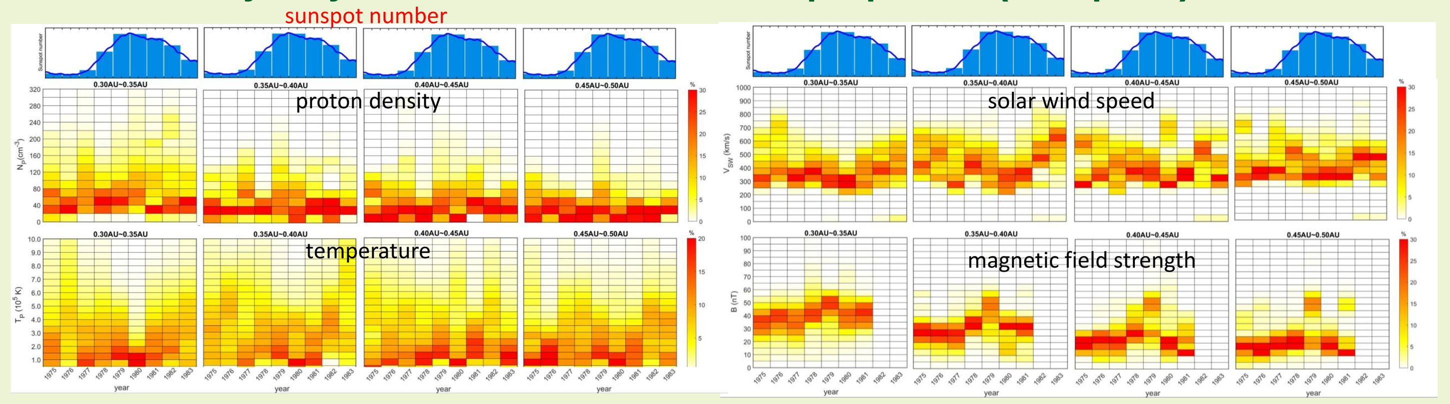

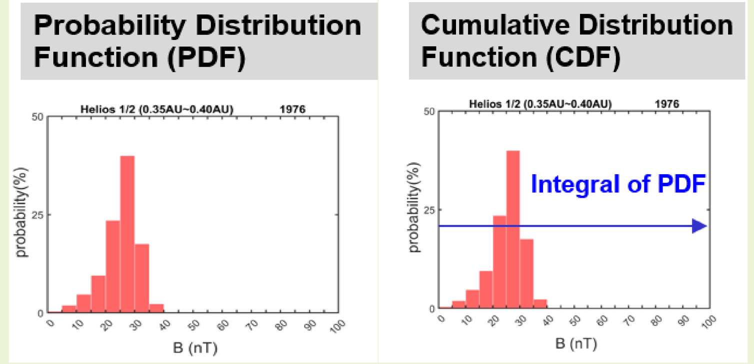

This study has been published in ApJ.
Lai, S. H., Yang Y.-H.*, and Ip W.-H. (2024), Magnetohydrodynamic Perspective on the Disappearance of Mercury's Bow Shock by Helios Data Exploration, The Astrophysical Journal, 961(1), 83, doi:10.3847/1538-4357/ad0a8a.

Temporal and Spatial Solar Wind Properties vs. M_F

yearly distribution of M_F PDF plots

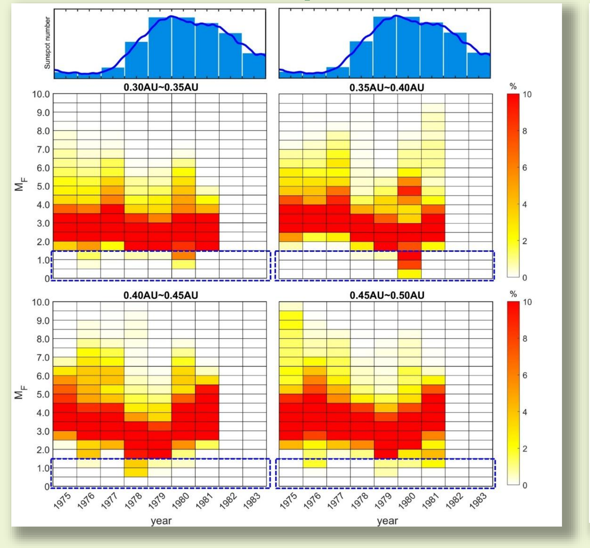

yearly distribution of M_F CDF plots

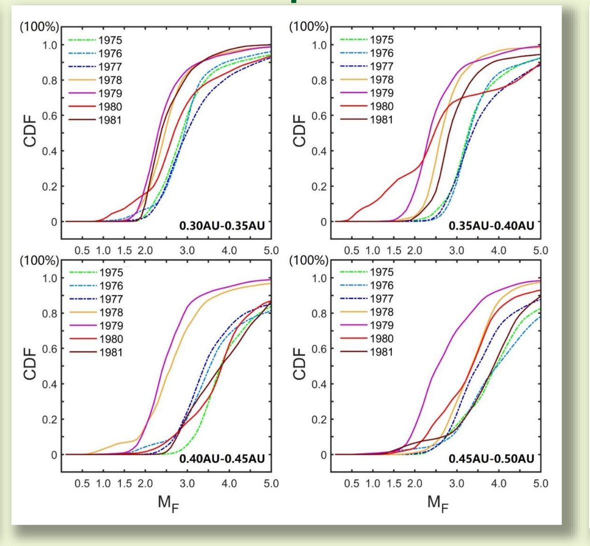

solar wind properties for M_F >1.5 and M_F ≤1.5 CDF plots

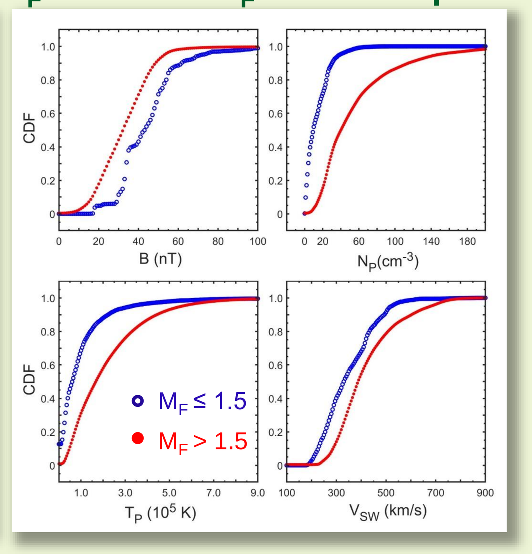

Bow shock cannot be generated by the fast-mode waves when M_F < 1.0 :
Extremely Low Fast-Mode Mach Number is defined as $M_F \le 1.5$

Selected Extremely Low M_F Events ($M_F \le 1.5$)

Inside the main body of an ICME

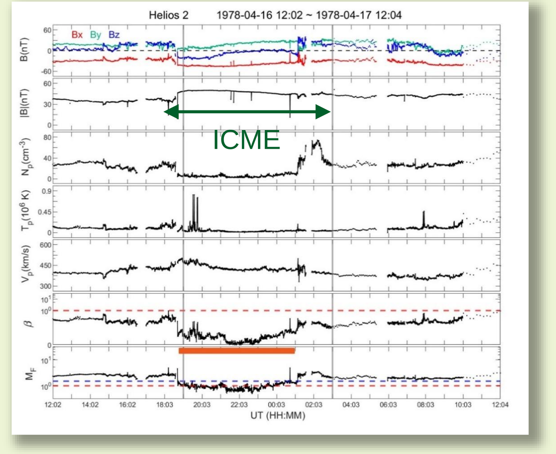

Beside an ICME

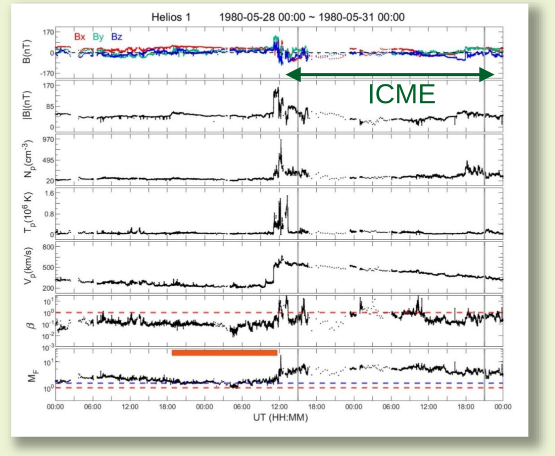

No ICME but a CIR

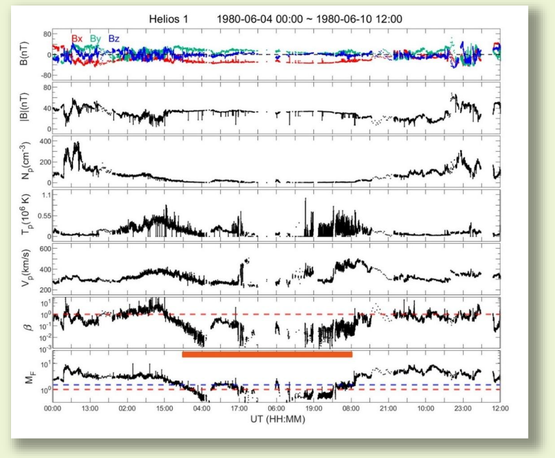

extremely low-M_F solar wind interval

Theoretical Model and MHD Simulation

group velocity of MHD waves | MHD simulations for a moving source | Schematic variety of Mercury's bow shock

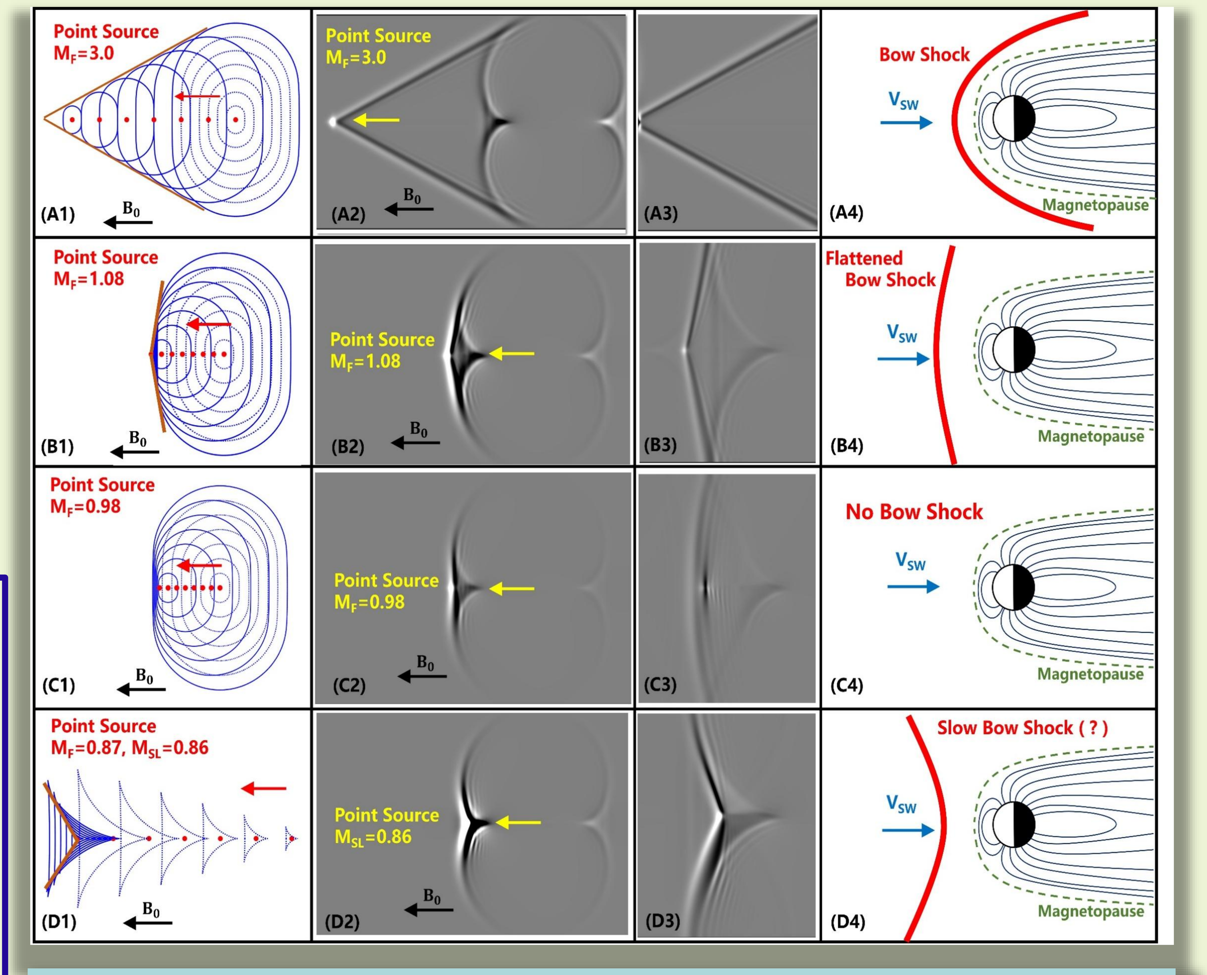

- *Anomalies in the interaction between the solar wind and the magnetosphere occur without a bow shock.*
- *Do the ICMEs dominate the occurrence of the extremely low-M_F interval?*

Kelvin-Helmholtz Instability at Mercury

KHI Evolution for heavily mass-loaded Mercury's magnetosphere (H) weakly mass-loaded Mercury's magnetosphere (W)

Initial Conditions

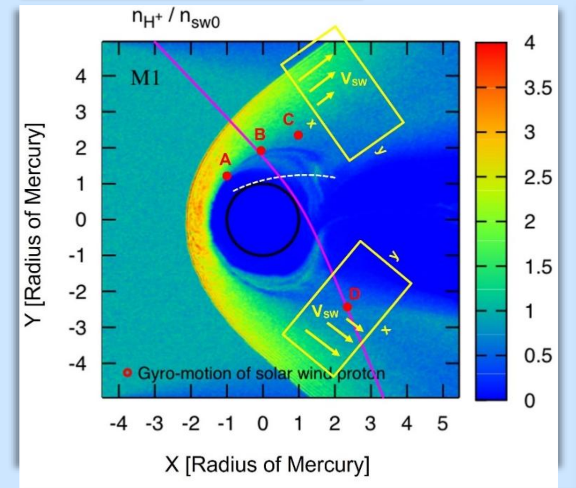

Global hybrid simulation for MESSENGER's first flyby of Mercury (Wang et. al, 2010)

Case		X_{MSO} (R_M)	n_{p01} (cm^{-3})	n_{p02} (cm^{-3})	θ_{01}	θ_{02}	B_{01} (nT)	B_{02} (nT)	V_{0y1} (km/s)	V_{0y2} (km/s)
A	H	+1.0	80.00	40.00	76°	90°	70.00	101.00	285.00	0.00
	W			0.8						
B	H	0	64.00	32.00	69°	90°	45.00	70.00	362.00	0.00
	W			1.5						
C	H	-1.0	44.80	18.00	67°	80°	36.00	56.00	395.00	0.00
	W			0.45						
D	H	-2.5	38.40	6.00	66°	60°	20.00	11.00	-400.00	0.00
	W			0.40						

2D MHD Simulation Results

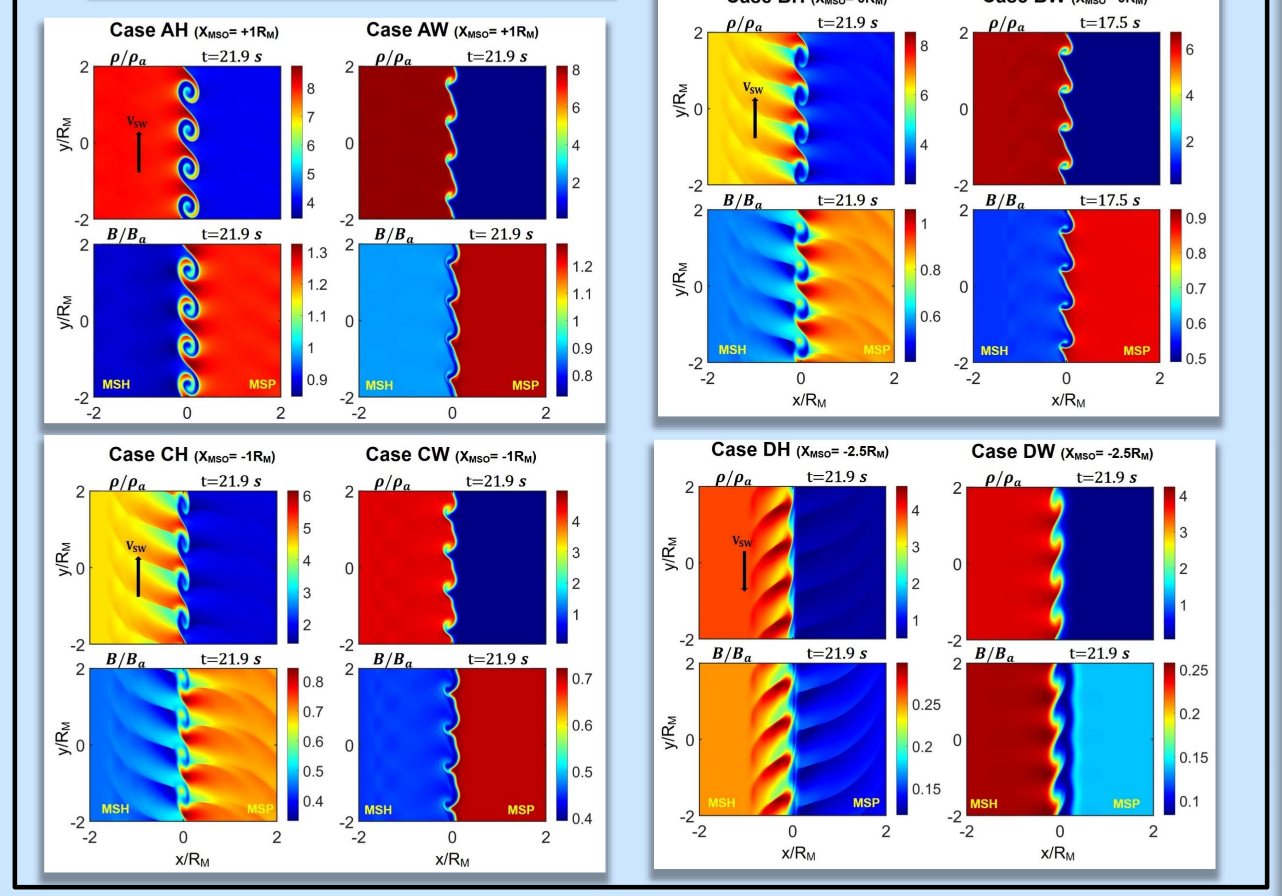

KHI Evolutions Under Two Scenarios

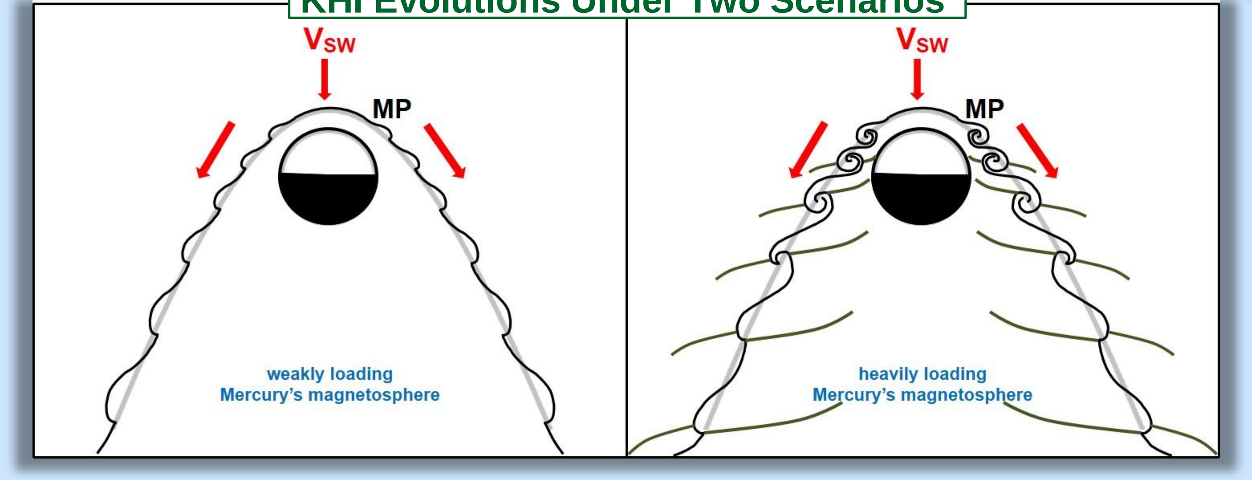

Energy and Momentum Transport

MHD Energy Equation

$$\underbrace{\frac{\partial}{\partial t}\left(\frac{1}{2}\rho V^2+\frac{3p}{2}+\frac{B^2}{2\mu_0}\right)}_{\text{Energy density } E}+\nabla\cdot\underbrace{\left[\left(\frac{1}{2}\rho V^2+\frac{5p}{2}+\frac{B^2}{\mu_0}\right)\mathbf{V}-\frac{\mathbf{B}(\mathbf{B}\cdot\mathbf{V})}{\mu_0}\right]}_{\text{Energy flux } \mathbf{W}}=0$$

MHD Momentum Equation

$$\frac{\partial}{\partial t}(\rho V)+\nabla\cdot\left(\rho VV-\frac{BB}{\mu_0}\right)+\nabla\left(p+\frac{B^2}{2\mu_0}\right)=0$$

Momentum flux: $\mathbf{S}=\rho\mathbf{VV}+\left(p+\frac{B^2}{2\mu_0}\right)\mathbf{1}-\frac{\mathbf{BB}}{\mu_0}$

$$S_{xy}=\hat{x}\cdot\mathbf{S}\cdot\hat{y}=\rho V_xV_y-\frac{B_xB_y}{\mu_0}\sim\mu\frac{dV_y}{dx},$$ μ: viscosity

For Perturbations

$$\mathbf{W}=\mathbf{W}_0+\delta\mathbf{W}$$
$$E=E_0+\delta E$$
$$\mathbf{S}=\mathbf{S}_0+\delta\mathbf{S}$$
$$\delta W_x=\delta\mathbf{W}\cdot\hat{x}$$
$$\delta W_y=\delta\mathbf{W}\cdot\hat{y}$$
$$\delta S_{xy}=\hat{x}\cdot\delta\mathbf{S}\cdot\hat{y}$$

S_{xy} is also called the tangential stress (viscous shear stress)
ρV_xV_y : Reynold stress, $-\frac{B_xB_y}{\mu_0}$: Maxwell stress

	x≈0.5 R_M (Near Magnetopause)					x≈1.5 R_M (Inner Magnetosphere)				
	δW_x^{max} (erg/cm^2s)	δW_y^{max} (erg/cm^2s)	δS_{xy}^{max} (nP_a)	$\frac{\delta E^{max}}{E_{sw0}}$ (%)	$\frac{\delta S_{xy}^{max}}{D_{sw0}}$ (%)	δW_x^{max} (erg/cm^2s)	δW_y^{max} (erg/cm^2s)	δS_{xy}^{max} (nP_a)	$\frac{\delta E^{max}}{E_{sw0}}$ (%)	$\frac{\delta S_{xy}^{max}}{D_{sw0}}$ (%)
Case AH	9.3×10^{-2}	9.1×10^{-2}	4.2×10^{-3}	9.4	$\sim10^{-2}$					
Case AW	8.5×10^{-2}	7.1×10^{-2}	6.9×10^{-4}	6.2	$\sim10^{-3}$					
Case BH	7.6×10^{-2}	8.6×10^{-2}	6.1×10^{-3}	6.4	$\sim10^{-2}$	2.0×10^{-2}	1.7×10^{-2}	1.1×10^{-3}	1.5	$\sim10^{-2}$
Case BW	8.8×10^{-2}	7.6×10^{-2}	2.6×10^{-4}	5.8	$\sim10^{-3}$	1.2×10^{-2}	7.8×10^{-4}	7.0×10^{-7}	0.5	$\sim10^{-6}$
Case CH	5.8×10^{-2}	6.3×10^{-2}	6.2×10^{-3}	5.6	$\sim10^{-2}$	1.6×10^{-2}	1.5×10^{-2}	2.0×10^{-3}	1.8	$\sim10^{-2}$
Case CW	4.5×10^{-2}	5.1×10^{-2}	3.8×10^{-3}	5.3	$\sim10^{-3}$	1.4×10^{-2}	7.8×10^{-4}	6.5×10^{-6}	0.9	$\sim10^{-5}$
Case DH	1.1×10^{-2}	3.1×10^{-2}	4.3×10^{-3}	3.7	$\sim10^{-1}$	1.4×10^{-2}	1.3×10^{-2}	3.8×10^{-3}	2.8	$\sim10^{-2}$
Case DW	2.3×10^{-2}	1.8×10^{-2}	1.8×10^{-3}	3.5	$\sim10^{-2}$	6.3×10^{-3}	3.6×10^{-4}	5.5×10^{-6}	0.7	$\sim10^{-5}$

E_{sw0}: initial solar wind energy density
D_{sw0}: initial solar wind dynamic pressure

- ***The KHI with a heavily-loaded magnetosphere can efficiently transport momentum and energy away from the magnetopause in the presence of the fast-mode plane waves.***
- ***We estimate that the KHI at Mercury's magnetopause is a significant source of energy storage within the magnetosphere.***

This study has been published in ApJ.
Lai, S. H., Y.-C. Wang, Yang Y.-H.*, and Ip W.-H. (2024), Solar Wind – Magnetosphere Coupling by the Kelvin-Helmholtz Instability at Mercury, The Astrophysical Journal, 977(2), 266, doi:org/10.3847/1538-4357/ad944b.